Applied Radiation and Isotopes 68 (2010) 1846–1854

Contents lists available at ScienceDirect

Applied Radiation and Isotopes

journal homepage: www.elsevier.com/locate/apradiso

Isotopic noble gas signatures released from medical isotope production facilities—Simulations and measurements

Paul R.J. Saey [a,*], Theodore W. Bowyer [b], Anders Ringbom [c]

[a] Vienna University of Technology, Atomic Institute of the Austrian Universities, Stadionallee 2, 1020 Vienna, Austria
[b] Pacific Northwest National Laboratory (PNNL), P.O. Box 999, Richland, WA 99352, USA
[c] Swedish Defence Research Agency (FOI), Defence and Security, Systems and Technology Division, 172 90 Stockholm, Sweden

ARTICLE INFO

Article history:
Received 24 December 2009
Received in revised form
12 February 2010
Accepted 5 April 2010

Keywords:
Uranium target irradiation
Medical isotopes
Low level radioxenon measurement
Environmental monitoring
Treaty verification
CTBTO

ABSTRACT

Radioxenon isotopes play a major role in confirming whether or not an underground explosion was nuclear in nature. It is then of key importance to understand the sources of environmental radioxenon to be able to distinguish civil sources from those of a nuclear explosion. Based on several years of measurements, combined with advanced atmospheric transport model results, it was recently shown that the main source of radioxenon observations are strong and regular batch releases from a very limited number of medical isotope production facilities.

This paper reviews production processes in different medical isotope facilities during which radioxenon is produced. Radioxenon activity concentrations and isotopic compositions are calculated for six large facilities. The results are compared with calculated signals from nuclear explosions. Further, the outcome is compared and found to be consistent with radioxenon measurements recently performed in and around three of these facilities. Some anomalies in measurements in which ^{131m}Xe was detected were found and a possible explanation is proposed. It was also calculated that the dose rate of the releases is well below regulatory values.

Based on these results, it should be possible to better understand, interpret and verify signals measured in the noble gas measurement systems in the International Monitoring of the Comprehensive Nuclear-Test-Ban Treaty.

© 2010 Elsevier Ltd. All rights reserved.

1. Introduction

1.1. Radioxenon monitoring

The Comprehensive Nuclear-Test-Ban Treaty (CTBT) bans all nuclear explosions in all environments. Its verification is based on the detection, identification and localisation of possible nuclear explosions (UNGA, 1996; Dahlman et al., 2009). Near real-time noble gas monitoring, together with five other technologies (radionuclide particulate measurements, seismic, hydroacoustic, infrasound and atmospheric transport modelling), is able to detect, identify and locate them.

The International Monitoring System (IMS) is part of the verification system of the CTBT. According to this treaty there will be at its Entry-Into-Force (EIF) 40 stations worldwide capable of measuring the relevant noble gases (protocol to the CTBT, Part 1, C, 10) with a sensitivity for ^{133}Xe better than 1 mBq/m^3. The CTBT relevant isotopes are ^{131m}Xe ($t_{1/2}$=11.9 days), ^{133m}Xe (2.19 days), ^{133}Xe (5.243 days) and ^{135}Xe (9.14 h). These isotopes have sufficiently high abundances and suitable half-lives for use as CTBT verification tracers: radionuclides with half-lives too short to decay away before reaching a monitoring station and isotopes with long half-lives have a too low specific activity to be measured.

Since their deployment, the IMS noble gas systems have collected worldwide more than 20,000 daily and 12 h environmental samples, in which the radioxenon content was measured. By late 2010, there should be 28 IMS radionuclide stations around the globe that will be equipped with noble gas monitoring technology.

After the announced nuclear explosion in the Democratic People's Republic of Korea (DPRK) in October 2006, the Swedish Defence Research Agency (FOI) confirmed using the airborne activity ratio ^{133m}Xe/^{133}Xe, which was measured in the Republic of Korea, that the explosion was nuclear (Ringbom et al., 2007, 2009). Also the increased ^{133}Xe activity concentration measured at the Yellowknife IMS station in North Canada in late October 2006 was consistent with the leak scenarios assumed for a low yield underground nuclear explosion on the Korean peninsula (Saey et al., 2007). This demonstrates the importance of two factors: radioxenon activity concentration ratios can identify the nuclear origin of a source if several isotopes are measured and the

* Corresponding author. Tel.: +43 1 58801 14168.
E-mail address: paul.saey@ati.ac.at (P.R.J. Saey).

0969-8043/$ - see front matter © 2010 Elsevier Ltd. All rights reserved.
doi:10.1016/j.apradiso.2010.04.014

knowledge of the radioxenon background can help identify such an event even in the case that only one isotope is detected.

Careful analysis of IMS data has shown that the major sources for the measured global radioxenon background appear to be environmental releases from medical isotope production facilities (MIPFs) producing mostly ^{99}Mo ($t_{1/2}$=65.94 h) and ^{131}I ($t_{1/2}$= 8.04 days) (Hoffman et al., 2009; Saey, 2009; Wotawa et al., 2009) with activity ratios very similar to nuclear explosions.

In this paper, these isotopic ratios are discussed, using calculations as well as observations. Radioxenon production in general and in MIPFs in particular are discussed in Sections 1.2 and 1.3, respectively. Section 2 is devoted to a description of simulations of radioxenon production in MIPF's, and the calculations are compared to data from different facilities in Section 3. The particular question of influence from ^{131}I on the radioxenon ratios is discussed in Section 4, and the paper ends with discussion and conclusions in Section 5.

1.2. Radioxenon production

Radioxenon isotopes are created during the fission of heavy nuclei, such as ^{235}U, but also during nuclear reactions, such as (n,p) reactions. In addition to nuclear explosions, they can also be created in, among others, nuclear power plants (NPP), nuclear research reactors or medical isotope production facilities.

Approximately 15% of the yield from uranium or plutonium fission are noble gases, mainly xenon isotopes with atomic masses around 130. Fig. 1 and Table 1 show the isobaric decay chains for the masses 131, 133 and 135. The radioxenon isotopes created during uranium fission are produced either directly as fission products or indirectly through decay of higher mass fission products. The number of atoms produced as fission products per fission is the direct (or "independent") fission yield, whereas the cumulative (or "chain") fission yield is defined as the total number of atoms of a certain isotope produced, including both direct production and decay.

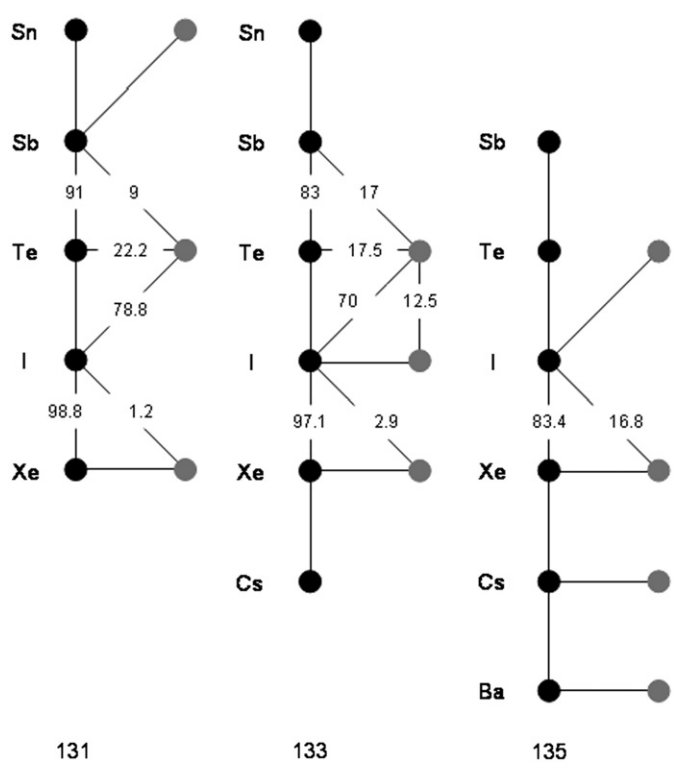

Fig. 1. Isobaric decay chains for the masses 131, 133 and 135 with the branching ratios (in %) according to Table 1—the grey dots are metastable states (isomers).

Table 1 shows the half-life, branching ratios, cumulative and direct fission yield for the nuclides of the relevant radioxenon mass chains, which will be used in the further presented calculations. The former two originate from the Evaluated Nuclear Structure Data File (ENSDF, 2009) and the latter two from the compilation of fission yields by England and Rider (1994).

In this work, only thermal neutrons (0.0253 eV) were considered when simulating target irradiation, since thermal neutron induced fission dominates the fission product production process.

Understanding the isotopic ratios expected from different processes is crucial when trying to distinguish nuclear explosions (where the irradiation occurs within microseconds) from MIPFs (where the irradiation is performed for several days) and from nuclear power plants (where the uranium irradiation time is on the order of months to years). Each radioxenon source has to be studied thoroughly to understand on the one hand the total amount of radioxenon isotopes that are created in fission and then released, and on the other hand its isotopic composition. In addition, in some of the processes, parent radionuclides such as radioiodine contribute to the radioxenons and affect the ratios. This is particularly true for reactor-produced radioxenon (Bowyer et al., 2002).

1.3. Radioxenon isotopes in medical isotope production

Four large and two smaller medical isotope production facilities that export internationally are known: Chalk River Laboratories (CRL, Chalk River, Canada), Covidien Radiopharmaceuticals/Nuclear Research and Consultancy Group (NRG, Petten, The Netherlands), l'Institut des Radioéléments (IRE, Fleurus, Belgium) and Nuclear Technology Products (NTP, Pelindaba, South Africa) as well as the Australian Nuclear Science and Technology Organisation (ANSTO, Lucas Heights, Australia) and the Comisión Nacional de Energía Atómica (CNEA, Buenos Aires, Argentina) (see Table 2).

The most common and efficient way to produce ^{99}Mo for medical applications is by neutron irradiation of highly enriched uranium (HEU; uranium with up to 93% of ^{235}U) or low enriched uranium (LEU; uranium with less than 20% ^{235}U). According to IAEA (2009) this process is used in around 95% of the globally produced ^{99}Mo.

Uranium targets for the production of radioisotopes, typically consisting of uranium metal assembled between two aluminium plates, are irradiated in a nuclear reactor for 2–12 days using a thermal neutron flux between 10^{13} and 5×10^{14} n/cm^2 s. The irradiation time is a compromise between the production of the isotopes of interest, which approaches diminishing returns after a few days, and the formation of undesirable isotope by-products. After irradiation, the targets are left to decay for typically 24 h (see Table 3) to remove short-lived isotopes in order to reduce the total dose rate. The uranium is then dissolved in a hot-cell using an acid or a base. During the dissolution process, which takes approximately 1–2 h, the noble gases created during fission or subsequent decay are released and processed in varying ways. The other fission products are separated and purified (see Fig. 2).

Depending on the facility, some noble gases are recovered and carried with helium to krypton, xenon and/or iodine recovery cells (Salacz, 1985). In these cells, the gases are frozen out from the carrier using liquid nitrogen, and are separated from each other during warming, by adsorption on molecular sieves and trapping on copper clippings. Finally, they are purified and shipped to the end customer. At other facilities, the noble gases are treated as waste. These facilities use charcoal delay lines to reduce the activity before being released to the atmosphere.

Table 1
Isotopic data used in the calculations presented in this paper. The cross sections in the last column are thermal (0.0253 eV) cross sections for neutron capture (n, γ) producing a ground level isotope. The CTBT relevant isotopes are marked in boldface.

Fission product	Half-life	$^{235}U_{thermal}$ cumulative fission yield (%)	$^{235}U_{thermal}$ direct fission yield (%)	Branching factor for β−decay to a 1st level metastable state isotope	Branching factor for β−decay to a ground state isotope	Isomeric transition	Thermal cross sections [Barn]
Tin-131	0.650 min	9.06E−01	8.81E−01	0	1	0	0
Tin-131m	1.020 min	0.00E+00	0.00E+00	0	1	0	0
Tin-133	0.024 min	1.38E−01	1.38E−01	0	1	0	0
Antimony-131	23 min	2.56E+00	1.65E+00	0	1	0	0
Antimony-133	2.5 min	2.40E+00	2.26E+00	0	1	0	0
Antimony-135	0.029 min	1.46E−01	1.45E−01	0	1	0	0
Tellurium-131	25 min	2.55E+00	9.70E−02	0	1	0	0
Tellurium-131m	32.4 h	4.12E−01	2.33E−01	0	0.778	0.222	0
Tellurium-133	12.4 min	3.06E+00	1.15E+00	0	1	0	0
Tellurium-133m	55.4 min	3.99E+00	2.99E+00	0	0.83	0.17	0
Tellurium-135	0.317 min	3.34E+00	3.22E+00	0	1	0	0
Iodine-131	8.04 d	2.89E+00	3.92E−03	0.011777	0.988223	0	0.7
Iodine-133	20.8 h	6.70E+00	1.65E−01	0.028	0.972	0	0
Iodine-133m	0.150 min	0.00E+00	0.00E+00	0	0	1	0
Iodine-135	6.570 h	6.28E+00	2.93E+00	0	1	0	0
Xenon-131	stable	2.89E+00	1.42E−07	0	0	0	90
Xenon-131m	11.9 day	4.05E−02	3.48E−07	0	0	1	0
Xenon-133	5.243 day	6.70E+00	6.66E−04	0	1	0	200
Xenon-133m	2.19 day	1.89E−01	1.89E−03	0	0	1	0
Xenon-135	9.14 h	6.54E+00	7.85E−02	0	1	0	2.6E+06
Xenon-135m	15.3 min	1.10E+00	1.78E−01	0	0.00004	0.99996	0
Cesium-133	stable	6.70E+00	7.92E−07	0	0	0	27
Cesium-135	2.30E+06y	6.54E+00	4.91E−04	0	1	0	8.7
Cesium-135m	53 min	0.00E+00	0.00E+00	0	0	1	0
Barium-135	stable	6.54E+00	7.64E−08	0	0	0	6
Barium-135m	28.8 h	0.00E+00	0.00E+00	0	0	1	0

Table 2
The different facilities discussed in this paper and the references in the literature on their specific processing parameters.

Facility operator		Location	Country	Refs.
ANSTO	Australian Nuclear Science and Technology Organisation	Lucas Heights	Australia	Tinker et al. (2010); Saey et al. (2010)
CNEA	Comisión Nacional de Energia Atómica	Buenos Aires	Argentina	IAEA (1989)
CRL	Chalk River Laboratories	Chalk River	Canada	IAEA, (1989)
IRE	Institut des Radioéléments	Fleurus	Belgium	Salacz (1985); Bonet et al. (2005)
NRG	Nuclear Research and Consultancy Group	Petten	The Netherlands	pers. comm. Dr. A.A. Sameh
NTP	Nuclear Technology Products Radioisotopes Pty.	Pelindaba	South Africa	IAEA (1989); Le Roux (1991); Ball (1999)

Table 3
Parameters used for the irradiation of uranium targets for medical isotope production at different facilities.

Target parameters	ANSTO	CNEA	CRL	IRE	NRG	NTP
^{235}U enrichment (%)	19.75	19.70	93.00	93.00	93.00	46.00
Total uranium (g)	12.66	7.20	2.40	4.52	5.38	15.54
^{235}U weight (g)	2.50	1.40	2.23	4.20	5.00	7.15
Al weight (g)		16.50	36.00	30.00		26.46
Neutron flux (n/cm^{2}s)	9.0×10^{13}	1.5×10^{14}	2.5×10^{14}	1.5×10^{14}	1.5×10^{14}	1.5×10^{14}
Min. irradiation time (h)	72	72	150	100	−144	50
Max. irradiation time (h)	336	168	280	150	−144	200
Cooling time (h)	9–14			36	20	24–200
Average number of targets dissolved per batch	8	9	10	2×6	12	12

NTP and NECSA plan to change to LEU targets.

2. Simulation of radioxenon in medical isotope production

2.1. Method

Detailed open literature on the details of the isotope production in MIPFs is limited but some data are available. Table 2 gives an overview of the six above mentioned facilities. This paper will, based on the available information, present calculations for each of these facilities. Further, the possible CTBT relevant radioxenon isotopes' activity created and their isotopic compositions are calculated.

Using the information from Tables 1 and 3, the produced radioxenon activity for the minimum (3 days) and maximum (10 days) irradiation time was calculated for each site. The simulation tool used and adapted for these calculations was "Nuclear Analysis 2.0—Decay and Irradiation Software" (Vilece, 1996), assuming a pure thermal neutron flux. This software is designed to perform decay and irradiation calculations for ground

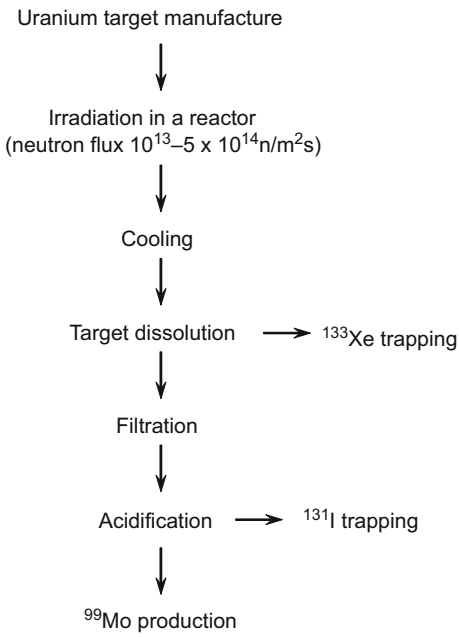

Fig. 2. A common technique for ^{99}Mo production.

and metastable state isotopes. The problems are solved numerically in order to account for time varying concentrations, flux conditions and the large number of nuclides linked by decay and/or neutron reactions. Some results were verified with calculations performed with "Scale 5.1/Origen-ARP" (ORNL, 2000) and the results were identical. All data presented in this paper originate from the Nuclear Analysis 2.0 software.

2.2. Radioxenon calculations in a medical isotope facility

The graphs in Fig. 3 show the resulting radioxenon activities for the two irradiation times studied, using the parameters of the ANSTO facility, as an example. Fig. 3a shows the activity of the four CTBT relevant radioxenon isotopes, as well as the short lived ^{135m}Xe as a function of time. Fig. 3b illustrates the ratio of the isotopes ^{131m}Xe, ^{133m}Xe and ^{135}Xe vs. ^{133}Xe as a function of time. Fig. 3c shows the isotopic ratios ^{135}Xe/^{133}Xe and ^{133m}Xe/^{133}Xe and Fig. 3d presents the isotopic ratios ^{135}Xe/^{133}Xe and ^{133m}Xe/^{131m}Xe. Using such ways of presenting the radioxenon isotopic ratios, Kalinowski and Pistner (2006) have calculated that nuclear reactors emit radioxenon with ratios that are situated left of the red dashed line in Fig. 3c and d (called the "discrimination line" in Kalinowski et al. (2010)). As can be seen in Fig. 5, the radioxenon ratios of nuclear explosion scenarios can be found in such graphs right of this discrimination line.

It is shown in Fig. 3c and d that the irradiation time is the main factor characterizing the ratios of the radioxenon production over time. The dashed lines show the activity or ratio after target dissolution, i.e. when xenon has been separated from all its precursors. The only nuclide that will continue to be produced is ^{133}Xe from ^{133m}Xe decay.

The simulation results in Table 4 show the maximum calculated activity of ^{133}Xe for all sites in Table 2. Furthermore, the ratios of the isotopes ^{131m}Xe, ^{133m}Xe and ^{135}Xe vs. ^{133}Xe, 5 days after the dissolution of the uranium targets, are shown. This is a realistic time frame for when the gases could reach an IMS noble gas station, although longer times are also possible.

Fig. 4 shows the 4-isotopic ratios, using the known minimum and maximum irradiation times (48 and 220 h) from possible uranium targets (HEU) used at the IRE facility in Belgium. The longer the targets are irradiated, the more the 3- and 4-isotopic ratios move to the left, which is towards the region of the nuclear power plants and away from the nuclear explosion area.

The same calculations were performed for LEU targets. The results are identical and overlap with the different graphs from Fig. 3. The same scenarios were also calculated for a lower neutron flux (1.5×10^{14} n/cm^2 s) and for a longer cooling time (200 h). These factors made no significant difference in the results shown in Fig. 3.

2.3. Radioxenon signatures in a nuclear explosion

For comparison, radioxenon activity ratios produced in two types of nuclear explosions, pure ^{235}U and pure ^{239}Pu, respectively, were calculated using Nuclear Analysis 2.0 with fast neutron spectra. The three- and four-isotopic ratios are presented in Fig. 5. Dashed lines indicate the ratios of the radioxenon isotopes when they are separated immediately after the explosion from the parent isotopes, which might be the case in an atmospheric nuclear explosion (full fractionation of the non-volatile products). The solid line shows the activity ratios for the case when all parent nuclides stay together, which could be the case inside the cavity of an underground nuclear explosion (no fractionation takes place).

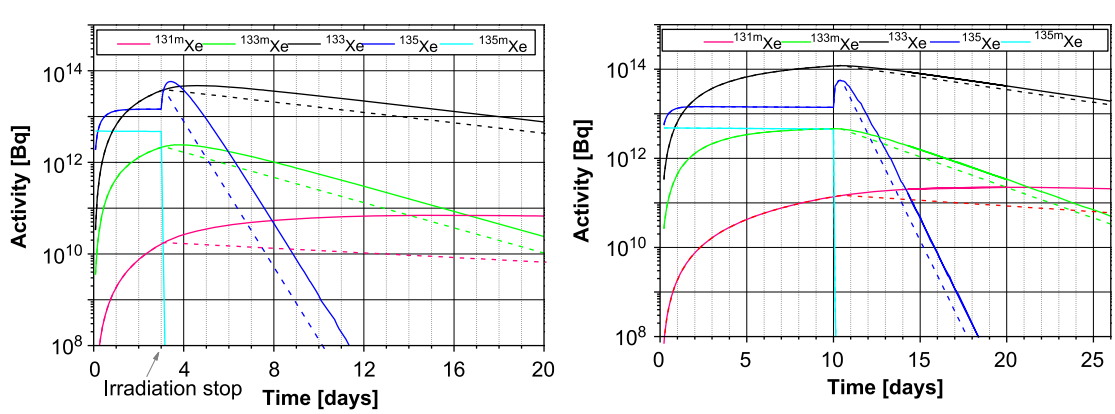

Fig. 3a. Simulations of radioxenon activity in irradiated targets over time from the ANSTO facility, as an example. The left panel shows the results for a 3 day irradiation and the right panel the results for a 10 day irradiation. The dashed lines show the activity for the case of the separation of the mother nuclides due to the chemical separation. (For interpretation of the references to colour in this figure legend, the reader is referred to the web version of this article.)

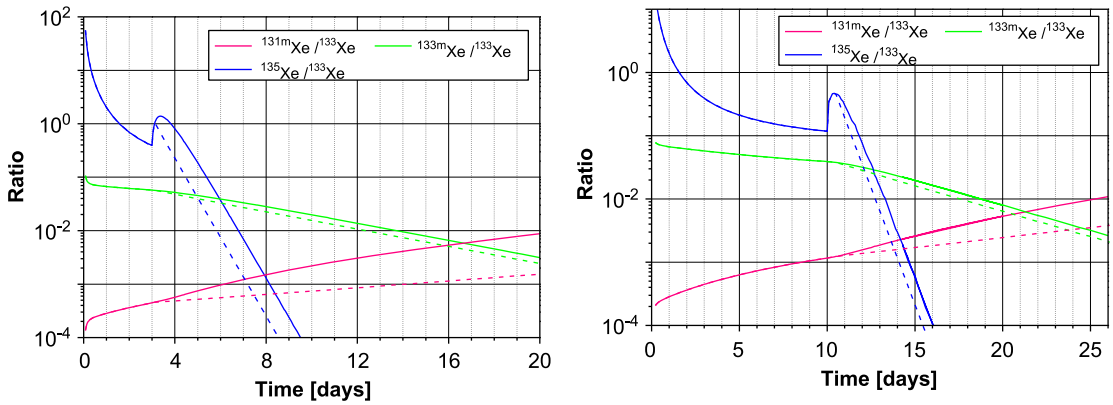

Fig. 3b. Simulations of radioxenon activity ratios over ^{133}Xe in irradiated targets over time from the ANSTO facility. The left panel shows the results for a 3 day irradiation and the right panel the results for a 10 day irradiation. The dashed lines show the activity concentration for the case of the separation of the mother nuclides due to the chemical separation.(For interpretation of the references to colour in this figure legend, the reader is referred to the web version of this article.)

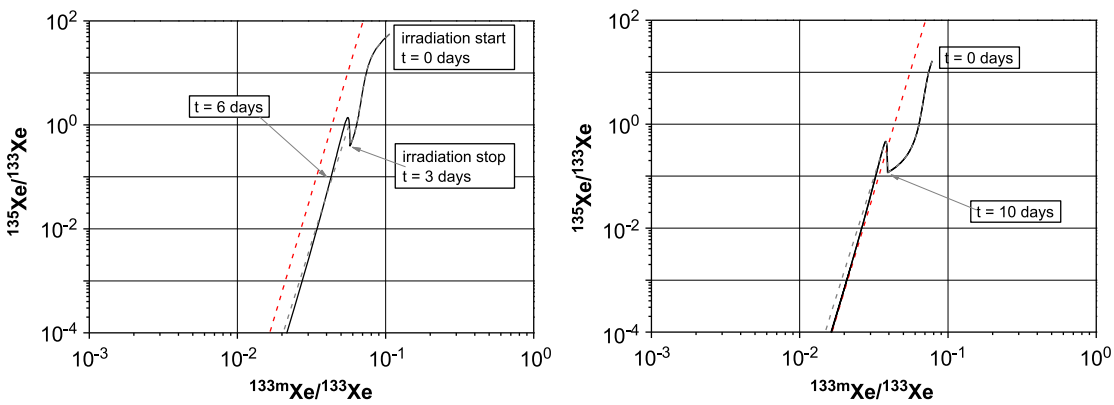

Fig. 3c. Simulations of radioxenon activity ratios (^{135}Xe/^{133}Xe vs. ^{133m}Xe/^{133}Xe) in irradiated targets from the ANSTO facility. The left panel shows the results for a 3 day irradiation and the right panel the results for a 10 day irradiation. The red dashed line indicates the discrimination line (left of it is the region where nuclear power plant activity ratios can be expected and right of it is the nuclear explosion region). The grey dashed line shows the activity for the case of the separation of the mother nuclides due to the chemical separation. (For interpretation of the references to colour in this figure legend, the reader is referred to the web version of this article.)

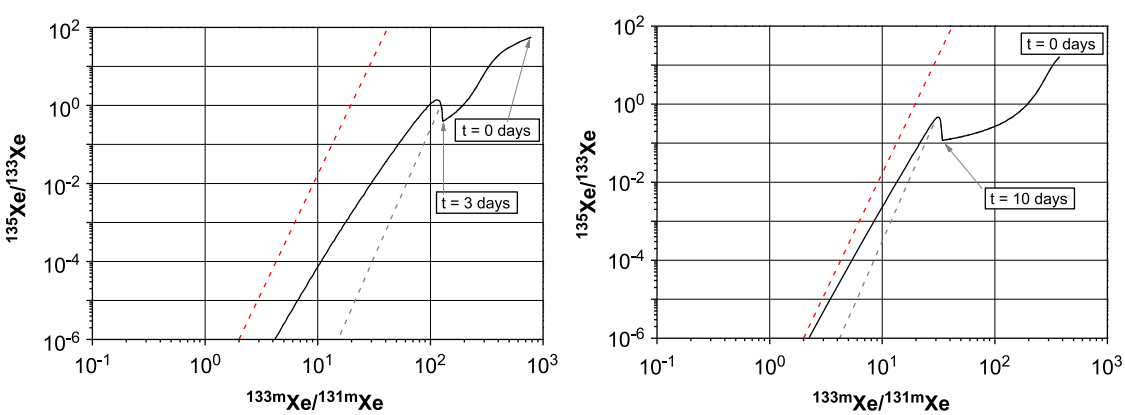

Fig. 3d. Simulations of radioxenon activity ratios (^{135}Xe/^{133}Xe vs. ^{133m}Xe/^{131m}Xe) in irradiated targets from the ANSTO facility. The left panel shows the results for a 3 day irradiation and the right panel the results for a 10 day irradiation. The red dashed line indicates the discrimination line (left of it is the region where nuclear power plant activity ratios can be expected and right of it is the nuclear explosion region). The grey dashed line shows the activity for the case of the separation of the mother nuclides due to the chemical separation. (For interpretation of the references to colour in this figure legend, the reader is referred to the web version of this article.)

Similar graphs for MIPFs, as shown in Fig. 3, illustrate the fact that atmospheric releases from MIPFs have the same signature as a nuclear explosion with a late separation (more than 1 day) of the radioxenon gases from the parent isotopes.

3. Comparison of environmental measurements with the simulations

Recently, field atmospheric measurement campaigns took place, where radioxenon in, around and remote from MIPFs was

Table 4
The maximum ^{133}Xe activity for several scenarios as well as the activity ratios of ^{131m}Xe, ^{133m}Xe and ^{135}Xe to ^{133}Xe, 5 days after the dissolution.

Facility (target irradiation time)	Maximum activity ^{133}Xe after irradiation stop (Bq)	^{131m}Xe/^{133}Xe ratio, 5 days after dissolution	^{133m}Xe/^{133}Xe ratio, 5 days after dissolution	^{135}Xe/^{133}Xe ratio, 5 days after dissolution
ANSTO (3 days)	4.8×10^{13}	1.5×10^{-3}	2.8×10^{-2}	1.5×10^{-3}
ANSTO (10 days)	1.2×10^{14}	2.6×10^{-3}	2.0×10^{-2}	6.0×10^{-4}
CNEA (5 days)	7.7×10^{13}	2.3×10^{-3}	2.0×10^{-2}	1.0×10^{-4}
CRL (6 days)	2.4×10^{14}	2.0×10^{-3}	2.3×10^{-2}	7.2×10^{-4}
IRE (2 days)	7.9×10^{13}	7.3×10^{-4}	2.9×10^{-2}	1.3×10^{-3}
IRE (9 days)	2.6×10^{14}	2.5×10^{-3}	2.1×10^{-2}	5.7×10^{-4}
NRG (6 days)	4.0×10^{14}	1.0×10^{-3}	1.9×10^{-2}	1.2×10^{-5}
NTP (7 days)	1.4×10^{12}	8.3×10^{-4}	4.5×10^{-2}	9.5×10^{-2}

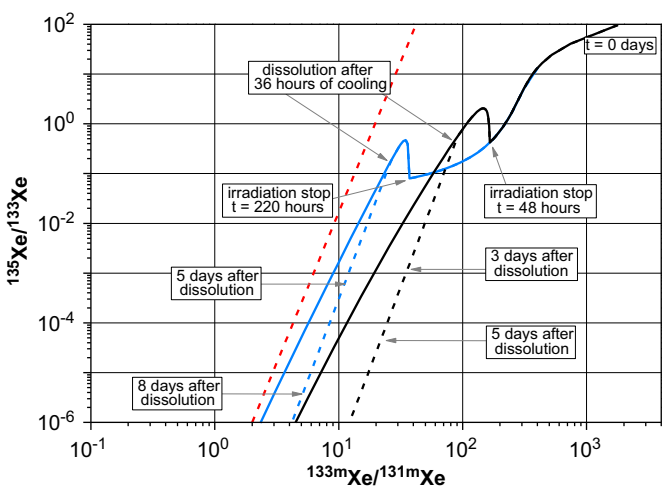

Fig. 4. An example of resulting isotopic ratios assuming short and long irradiation times of a HEU target, using the parameters for IRE in Table 3. The red dashed line is the proposed discrimination line (left nuclear power plants, right nuclear explosions). (For interpretation of the references to colour in this figure legend, the reader is referred to the web version of this article.)

measured with high sensitivity for the first time. In this section, these measured data will be compared with the calculations presented in the previous section.

3.1. Study of the Pelindaba facility, South Africa

Between 10 November and 22 December 2008, radioxenon was measured continuously with a SAUNA-II radioactive xenon measurement system in cooperation with the CTBTO and the Pacific Northwest National Laboratory (Richland, USA), at the North-West University, Mafikeng, South Africa, which is situated 250 km west of the Pelindaba NTP facility (Saey et al., 2009a). Fifty-six 12 h samples were measured with a SAUNA beta–gamma coincidence detector, of which 55 contained ^{133}Xe with values between 0.11 and 27.1 mBq/m^3. Eleven samples also contained ^{135}Xe and three samples ^{133m}Xe. The isotope ^{131m}Xe was not detected in any of the samples, which might indicate that the sampled air originated from a fresh release in which ^{131m}Xe has had no time to build up to measurable amounts.

Results from samples containing three radioxenon isotopes are shown in Fig. 6. In parallel, stack samples were taken at the NTP facility on an almost daily basis, in most cases shortly after the dissolution of the target. The samples were measured using an HPGe detector at the local laboratory of the South African Nuclear Energy Corporation (NECSA). As can be seen in Fig. 6, these measurements all fit well with the simulation. Ratios from stack measurements lower in the graph (i.e. longer decay time) originate from samples taken a longer time after the dissolution took place.

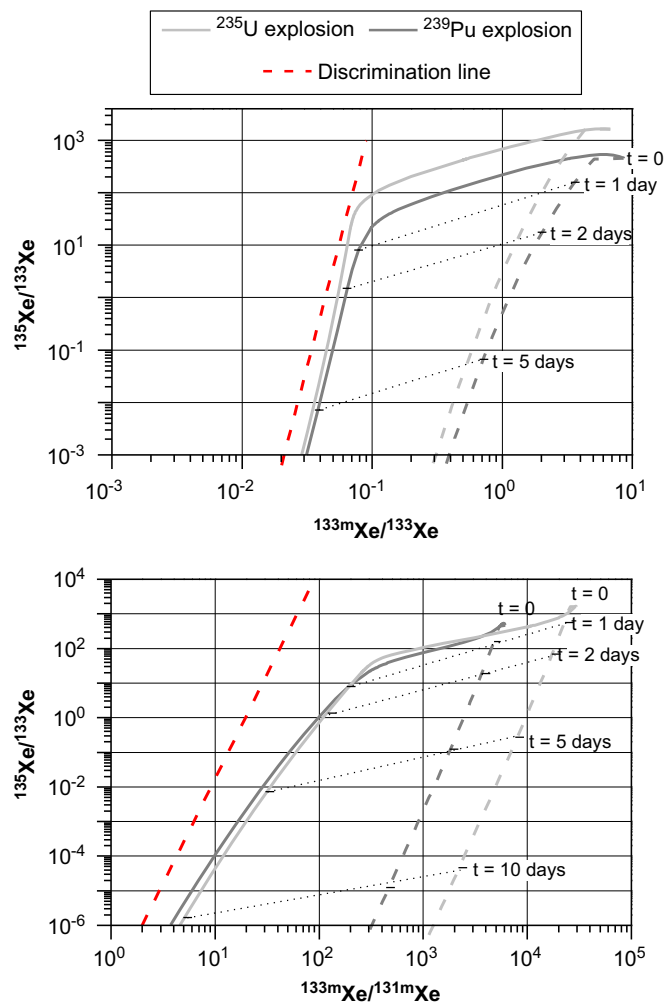

Fig. 5. Simulation of the isotopic ratios ^{135}Xe/^{133}Xe and ^{133m}Xe/^{133}Xe (top) and ^{135}Xe/^{133}Xe and ^{133m}Xe/^{131m}Xe (bottom) for a ^{235}U and for a ^{239}Pu explosion. The dashed line indicates the ratios in the case of immediate separation of the radioxenons from their parents. The time indicates the time after the detonation.

3.2. Study of the Fleurus facility, Belgium

During the summer of 2008, the CTBTO carried out in cooperation with the Swedish Defence Research Agency (FOI) a three-week field campaign in the region around the Belgian MIPF IRE in Fleurus, which is the third largest MIPF in the world (Saey et al., 2009b). The scope was to obtain the activity concentration of

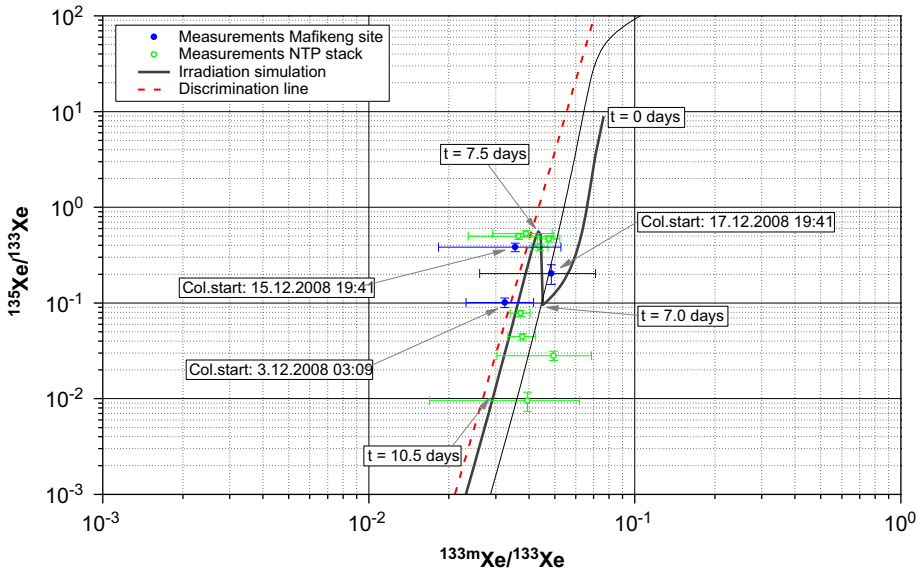

Fig. 6. A 3-isotopic graph of the simulation of radioxenon isotopes in HEU targets irradiated in the NTP facility. Red: proposed discrimination line (left nuclear power plants, right nuclear explosions, see Kalinowski et al., 2010), blue: environmental samples taken at Mafikeng, light green: stack samples at the NTP facility in Pelindaba and light grey: simulation of an HEU nuclear explosion. (For interpretation of the references to colour in this figure legend, the reader is referred to the web version of this article.)

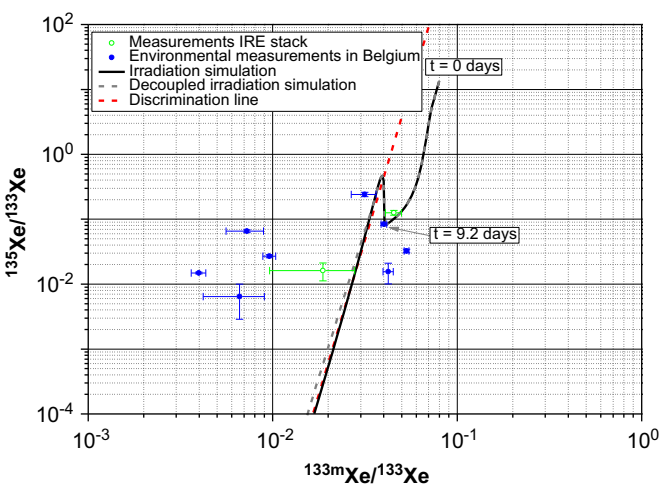

Fig. 7. A 3-isotopic graph of the simulation of radioxenon isotopes in HEU targets irradiated with the parameters common for the IRE facility. Red: discrimination line (left nuclear power plants, right nuclear explosions, see Kalinowski et al., 2010), blue: environmental samples taken in Belgium and light green: three stack samples from the IRE facility in Fleurus that contained the 3 isotopes. (For interpretation of the references to colour in this figure legend, the reader is referred to the web version of this article.)

the releases and the isotopic composition at different distances from the facility. Systematic "plume hunting" was performed during 3 weeks using a mobile SAUNA sampler in combination with meteorological forecasts. Thirty-five environmental and 3 stack samples from the IRE facility were measured at the FOI noble gas laboratory in Stockholm. Atmospheric ^{133}Xe concentrations in the range $0.7–4\times10^5$ mBq/m^3 were detected. The stack samples had concentrations in the range $2\times10^9–4\times10^{10}$ mBq/m^3.

The observed activity concentration ratios are shown together with the calculations in Fig. 7. It can be seen that some measurements are in good agreement with the simulations, but others are not. This might be explained with mixtures of gases produced in different processes inside the facility, like e.g., the fresh release after dissolution, the release of older radioxenon after the cleaning of the hot cells or the release of noble gases from waste storage tanks in which iodine is accumulated (De Coninck, pers. comm., 2009). The stack at the Fleurus facility is also used for the release of all air from the laboratories and hot cells belonging to two different companies (IRE and MDS Nordion) on the same premises. More information on the procedures used in the plant is needed to understand all measurement results in detail.

3.3. Study of the Lucas Heights facility, Australia

In November 2008, radioxenon isotopes were detected for the first time at the Melbourne (Australia) IMS station. Using atmospheric transport calculations, it was found that the detected concentrations of xenon originated from the MIPF ANSTO in Lucas Heights, near Sydney (Tinker et al., 2010; Saey et al., 2010). This medical isotope facility – the only one in Australia – started test production in late November 2008. Low enriched uranium targets (19.75% ^{235}U) are irradiated at the local new 20 MW Open Pool Australian Light-Water (OPAL) reactor and then dissolved. Other than the OPAL reactor itself, which is likely to have extremely low emissions compared to medical isotope production, there are no other known possible sources of radioxenon on the Australian continent.

Between 23 November 2008 and 4 February 2009, eight hot commissioning runs of the ^{99}Mo production facility were performed. Most emissions occurred on the first day of each of the runs and could be measured a few days later at the IMS station in Melbourne. No ^{131m}Xe was detected. Also here, the isotopical compositions of these long distance measurements are in agreement with the simulations (Fig. 8).

4. The influence of ^{131}I

When atmospheric radioxenon is measured, it is of key importance to understand how the measured isotopic mix can be interpreted to be able to understand its source. The mechanism for gas emissions can vary greatly, as is shown, e.g., in Fig. 7, with different processes in different facilities, different laboratories in the same facility and varying durations the noble gases will remain in certain parts of the facility. The radioxenon isotopes

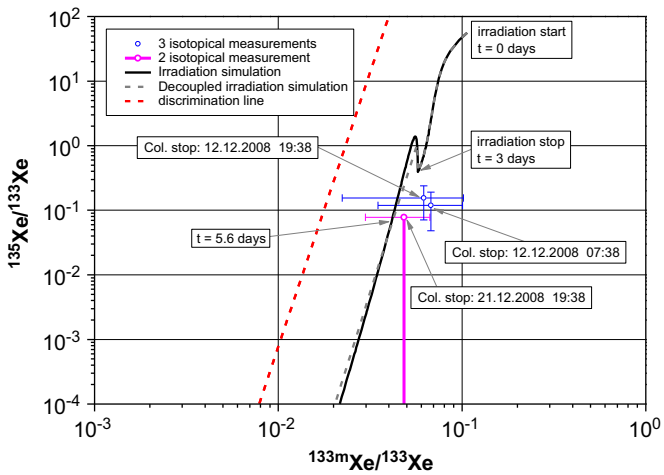

Fig. 8. A 3-isotopic ratio plot showing simulations and measurements of radioxenon isotopes produced in the ANSTO facility. Data are from three plumes passing the SAUNA system in Melbourne in November and December 2008. Blue: environmental samples having all three activity concentrations above the critical limit and magenta: environmental sample containing the ^{133m}Xe and ^{133}Xe isotopes above the critical limit, and using the MDC of ^{135}Xe as a maximum value. (For interpretation of the references to colour in this figure legend, the reader is referred to the web version of this article.)

themselves will behave in the same way in all facilities if they are not physically separated from each other, but the mixture within the facility and the decay dynamics vary in each of the decay chains and the xenon precursors (mostly iodine isotopes) are not inert gases and, therefore, are subject to the process used in the facility (acid/basic dissolution, immediate/delayed processing, etc.). At several facilities there is additional production of ^{131}I via the ^{130}Te(n,γ)^{131}Te process, followed by a β decay to ^{131m}Te, which then decays to ^{131}I. An amount of 1.2% of ^{131}I decays to ^{131m}Xe. Therefore, the xenon ratios expected outside of a facility may depend critically on how the xenon isotopes and their parents are treated in the facility.

Some facilities use the Cintichem process, in which the uranium targets are dissolved in nitric acid. Noble gases and volatized iodine are released together during uranium dissolution. A part will, therefore, also enter the stack, decay to ^{131m}Xe and join the already present other xenon isotopes.

Dissolving the uranium/aluminium targets in a basic solution will release the fission noble gases from the dissolver solution, but nearly all of the iodine remains in solution. In the next step, which can be performed several days later, lowering the pH of the solution will release iodine isotopes into the gas phase, allowing their separate recovery (as done by e.g., NRG).

When these gases will be measured in the environment, the added ^{131m}Xe from the other sources (liquid waste tanks, iodine created by neutron irradiation of ^{130}Te, etc.), if not filtered as well, will mix with the air and can lead to false conclusions in the 4-isotopic xenon plots shown above: the real radioxenon signal will be moved to the left site of the discrimination line and a potential signal that would be right of the line and therefore indicate a nuclear explosion, will move to the left and can be wrongly interpreted as a reactor signal.

5. Discussion and conclusions

Calculations were performed to examine the activity of four radioxenon isotopes, relevant to the verification of the CTBT, created during the irradiation of uranium targets used for the production of medical isotopes. It is shown that the neutron flux, the uranium enrichment of the targets and the cooling time of the targets after their irradiation have no major influence on the radioxenon activity ratios. The irradiation time of the targets and the use of delay lines (with a possible mixing of old and newly produced isotopes) do have a highly relevant effect that needs to be taken into account when analysing radioxenon data from MIPFs.

It should be noted that prevailing activity concentrations of a few mBq/m^3 of ^{133}Xe, as observed e.g., in Europe, yields low doses to human beings or other species in the biosphere. The dose rate factor of ^{133}Xe is about 5×10^{-8} mSv/y per mBq/m^3 (Kocher, 1980). This renders an annual dose to humans of many orders of magnitude less than what is caused by its more natural "cousins" radon-220 and 222 and their progeny, which is on average 1 mSv/y (UNSCEAR, 2009).

These calculations were compared with the results from three recently performed field campaigns conducted in the vicinity of, and inside the stack, of these facilities. The calculations are in good agreement with the environmental measurements. At one facility, however, several measurements differ considerably from the calculated ratios. One possible explanation is that several other activities that take place in that facility affect the isotopic ratios of the released noble gases. A good understanding of the different complex processes that occur in such facilities will help to model the releases more accurately.

Calculations of two different hypothetical nuclear explosions (pure fission of ^{235}U and ^{239}Pu) were compared with the releases from MIPFs. It is shown that the three- and four-isotope activity ratios from an explosion under certain circumstances (short irradiation period of the uranium target in the MIPF/separation of the radioxenons in an explosion after more than 1 day) are identical to the signals produced in an MIPF. It might therefore be suggested that for the sake of a stable verification system, longer irradiation of the targets in MIPFs would be useful. In addition, processes that reduce xenon emissions, such as the use of basic target dissolution processes, charcoal traps to collect and decay xenon isotopes more efficiently and careful operations including stack measurements to monitor emissions would be helpful. Sameh and Ache (1987) have shown that using an alkaline dissolution of the uranium targets instead of an acid one (as is done at the facility in Petten) reduces the releases significantly.

The four-isotopic activity ratio graph shown above has to be treated very carefully if it is to be used as a tool for discriminating nuclear explosions from civil radioxenon releases. As shown here, the signal from a nuclear explosion can move inside the non-explosive area by adding ^{131m}Xe. This isotope is a daughter of ^{131}I, which is a commonly used and widespread isotope that has several sources of creation and will therefore get mixed in the atmosphere with the possible nuclear explosion air. It should be reconsidered if this fourth radioxenon isotope has an additional value in the verification of the CTBT or if it is more misleading. In addition, the proposed discrimination line may have to be altered to account for the effects described in this work. For example, a second more horizontal discrimination line could help to discriminate between MIPF emissions and nuclear explosions by relying more heavily on ^{135}Xe/^{133}Xe.

Further conviviality and discussions between the verification community and the medical isotope production community are needed to continue the exchange of information to be able to explain all the detections in the global radioxenon monitoring network.

Disclaimer

The views expressed in this publication are those of the author and do not necessarily reflect the views of the Vienna University of Technology or any of the institutions mentioned herein.

Acknowledgements

The authors would like to thank Dr. Kenneth "Ken" Vilece and Dr. Anders Axelsson, both at IAEA in Vienna, for the very interesting and fruitful discussions on uranium target irradiation calculations. The authors appreciate Prof. Steve Biegalski and Dr. Derek Haas (both at the University of Texas) for interesting discussions and calculation comparisons. Prof. Arnaud Faanhof from NECSA (Pelindaba) is thanked heartily for measuring and providing the NTP stack sample data used in this paper. The anonymous reviewers are thanked for their fruitful comments and suggestions.

References

Ball, R.M., 1999. Characteristics of nuclear reactors used for the production of molybdenum-99. IAEA-TECDOC 1065, 5–17.

Bonet, H., David, B., Ponsard, B. 2005. Production of molybdenum-99 in Europe: status and perspectives. In: Proceedings of the 9th International Topical Meeting on Research Reactor Fuel Management, Budapest, April 2005.

Bowyer, T.W., Schlosser, C., Abel, K.H., Auer, M., Hayes, J.C., Heimbigner, T.R., McIntyre, J.I., Panisko, M.E., Reeder, P.L., Satorius, H., Schulze, J., Weiss, W., 2002. Detection and analysis of xenon isotopes for the comprehensive Nuclear-Test-Ban treaty international monitoring system. Journal of Environmental Radioactivity 59 (2), 139–151.

Dahlman, O., Mykkeltveit, S., Haak, H., 2009. Nuclear Test Ban—Converting Political Visions to Reality. Springer, Heidelberg 978-1-4020-6883-6.

England T.R., Rider B.F. 1994. Evaluation and compilation of fission product yields. LA-UR-94-3106, Los Alamos National Laboratory.

ENSDF, 2009. Evaluated Nuclear Structure Data File. National Nuclear Data Center, Brookhaven National Laboratory.

Hoffman, I., Ungar, K., Bean, M., Yi, J., Servranckx, R., Zaganescu, C., Ek, N., Blanchard, X., Petit, G.L., Brachet, G., Achim, P., Taffary, T., 2009. Changes in radioxenon observations in Canada and Europe during medical isotope production facility shut downs In 2008. Journal of Radioanalytical and Nuclear Chemistry 282 (3), 767–772.

IAEA, 1989. Fission molybdenum for medical use. IAEA-TECDOC, 515, International Atomic Energy Agency, Vienna.

IAEA, 2009. Nuclear technology review 2009. IAEA, Vienna, p. 46. 〈http://www.iaea.org/Publications/Reports/ntr2009.pdf3〉.

Kalinowski, M.B., Pistner, C., 2006. Isotopic signature of atmospheric xenon released from light water reactors. Journal of Environmental Radioactivity 88 (3), 215–235.

Kalinowski, M.B., Axelsson, A., Bean, M., Blanchard, X., Bowyer, T.W., Brachet, G., McIntyre, J.I., Peters, J., Pistner, C., Raith, M., Ringbom, A., Saey, P.R.J., Schlosser, C., Stocki, T.J., Taffary, T., Ungar, R.K., 2010. Discrimination of nuclear explosions against civilian sources based on atmospheric xenon isotopic activity ratios. Pure and Applied Geophysics 167, 4–5.

Kocher, D.C., 1980. Dose-rate conversion factors for external exposure to photon and electron radiation from radionuclides occurring in routine releases from nuclear fuel cycle facilities. Health Physics 38, 543.

Le Roux, J.S., 1991. Die produksie en kwaliteitskontrole van tegnesium-99m kitsstelle met spesiale verwysing na 'n kistsstel vir rooiselmerking. Ph.D. Thesis. Medicine, Universiteit van Stellenbosch, Stellenbosch, Rep. of South Africa.

ORNL, 2000. SCALE: a modular code system for performing standardized computer analyses for licensing evaluation. In Nureg/Cr-0200.

Ringbom, A., Elmgren, K., Lindh, K., 2007. Analysis of radioxenon in ground level air sampled in the Republic of South Korea on October 11–14, 2006. Report FOI-R-2273-SE, Swedish Defence Research Institute (FOI), Stockholm, Sweden.

Ringbom, A., Elmgren, K., Lindh, K., Peterson, J., Bowyer, T.W., Hayes, J.C., McIntyre, J.I., Panisko, M., Williams, R., 2009. Measurements of radioxenon in ground level air in South Korea following the claimed nuclear test in North Korea on October 9, 2006. Journal of Radioanalytical and Nuclear Chemistry 282 (1), 773–779.

Saey, P.R.J., 2009. The influence of radiopharmaceutical isotope production on the global radioxenon background. Journal of Environmental Radioactivity 100 (5), 396–406.

Saey, P.R.J., Ringbom, A., Bowyer, T.W., Becker, A., De Geer, L.-E., Nikkinen, M., Payne, R.F., 2009a. Understanding radioxenon isotopical ratios originating from radiopharmaceutical facilities. Geophysical Research Abstracts 11 EGU2009-9749-3.

Saey, P.R.J., Auer, M., Becker, A., Hoffmann, E., Nikkinen, M., Ringbom, A., Tinker, R., Schlosser, C., Sonck, M., 2010. The influence on the radioxenon background during the shut-down of three major radiopharmaceutical production facilities in the northern hemisphere and during the start-up of a radiopharmaceutical production facility in the Southern Hemisphere. Journal of Environmental Radioactivity JENVRAD-D-08-00192.

Saey, P.R.J., Bean, M., Becker, A., Coyne, J., d'Amours, R., De Geer, L.-E., Hogue, R., Stocki, T.J., Ungar, R.K., Wotawa, G., 2007. A long distance measurement of radioxenon in Yellowknife, Canada, in late October 2006. Geophysical Research Letters, 34 L20802.

Saey, P.R.J., Ringbom, A., Andersson, P., Ban, S., Becker, A., Elmgren, K., Camps, J., De Geer, L.-E., Lindh, K., Paquet, N., Peterson, J., Söderström, C., Sonck, M., Taffary, T., van der Meer, K., Verboomen, B., Zähringer, M., 2009b. Environmental characterisation of a major radioxenon source in Europe. Geophysical Research Abstracts 11 EGU2009-9182.

Salacz, J., 1985. Reprocessing of irradiated uranium 235 for the production of Mo-99, I-131, Xe-133 radioisotopes. Revue IRE Tijdschrift 9 (3), 22–28.

Sameh, A.A., Ache, H.J., 1987. Production techniques of fission molybdenum-99. Radiochimica Acta 41, 65–72.

Tinker, R., Orr, B., Grzechnik, M., Hoffmann, E., Saey, P.R.J., Solomon, S., 2010. Evaluation of radioxenon releases in Australia using atmospheric dispersion modelling tools. Journal of Environmental Radioactivity 101 (5), 353–361.

UNGA, 1996. United Nations General Assembly Resolution Number 50/245. UN, New York, USA.

UNSCEAR, 2009. Effects of ionizing radiation: United Nations Scientific Committee on the Effects of Atomic Radiation—UNSCEAR 2006 Report, Volume II—report to the general assembly, with scientific annexes C, D, and E—Annex E: sources-to-effects assessment for radon in homes and workplaces. Effects of ionizing radiation, 2, UNSCEAR, Vienna, Austria, p. 217.

Vilece, K., 1996. Nuclear Analysis 2.0, Decay and Irradiation Software. Vilece Consulting Inc., Vienna, Austria.

Wotawa, G., Becker, A., Kalinowski, M.B., Saey, P.R.J., 2009. Computation and analysis of the global distribution of the radioxenon background based on an emission inventory of nuclear power plants and other known major sources. Geophysical Research Abstracts 10A, A-03674.